Tear Proteomic Analysis From Offspring of Keratoconus Patients: New Insights Into Corneal Biomechanical Weakness and Disease Risk Stages

Maite López-López,[1,2] Uxía Regueiro,[1,2] Susana Bravo,[3] Carmen Pena,[3] Yaiza Pastoriza,[1,2] Mercedes Conde-Amboage,[4,5] Pablo Hervella,[6] and Isabel Lema[1,2,7]

[1]Corneal Neurodegeneration Group (RENOIR), Clinical Neurosciences Research Laboratory (LINC), Health Research Institute of Santiago de Compostela (IDIS), Santiago de Compostela, Spain
[2]Departamento de Ciruxía e Especialidades Médico-Cirúrxicas, Facultade de Óptica e Optometría, Universidade de Santiago de Compostela, Santiago de Compostela, Spain
[3]Proteomic Unit, Health Research Institute of Santiago de Compostela (IDIS), Santiago de Compostela, Spain
[4]Department of Statistics, Mathematical Analysis and Optimization, Universidade de Santiago de Compostela (USC), Spain
[5]CITMAga, Santiago de Compostela, Spain
[6]Neuroimaging and Biotechnology Group (NOBEL), Clinical Neurosciences Research Laboratory (LINC), Health Research Institute of Santiago de Compostela (IDIS), Santiago de Compostela, Spain
[7]Instituto Galego de Oftalmoloxía (INGO), Complexo Hospitalario Universitario de Santiago (CHUS), Santiago de Compostela, Spain

Correspondence: Isabel Lema, Corneal Neurodegeneration Group, RENOIR, Clinical neurosciences Research Laboratory, LINC, Hospital Clínico Universitario, Travesía da Choupana S/N, 15706- Santiago de Compostela 15706, Spain; mariaisabel.lema@usc.es.
Uxía Regueiro, Corneal Neurodegeneration Group, RENOIR, Clinical neurosciences Research Laboratory, LINC, Hospital Clínico Universitario, Travesía da Choupana S/N, 15706- Santiago de Compostela 15706, Spain; uxiaregueirolorenzo@gmail.com.

MLL and UR contributed equally to this work and share first authorship.

Received: December 17, 2024
Accepted: April 25, 2025
Published: May 28, 2025

Citation: López-López M, Regueiro U, Bravo S, et al. Tear proteomic analysis from offspring of keratoconus patients: New insights into corneal biomechanical weakness and disease risk stages. *Invest Ophthalmol Vis Sci.* 2025;66(5):41. https://doi.org/10.1167/iovs.66.5.41

Purpose. To analyze the tear proteome of keratoconus offspring (O-KC) and assess the molecular drivers underlying corneal biomechanical weakening at KC-risk stages.

Methods. This cross-sectional study included 80 O-KC young participants and 42 controls without a KC family history. Based on the corneal biomechanical behavior, O-KC eyes were classified as low, moderate, and high-risk of KC development (O-KC-LR, O-KC-MR, O-KC-HR). Tear fluid was extracted using Schirmer strips, and the proteomic profile was mapped using LC-MS/MS. Bioinformatic tools were used to determine the dysregulated protein's biological implications. The sensitivity-specificity of each biomarker for differentiating between controls and O-KC groups was determined. Logistic regression analysis (LRA) identified the optimal subset of predictors for modeling each biomechanical condition's probability.

Results. Twenty-nine percent of O-KC eyes showed moderate/high alterations in corneal biomechanical behavior. Fifteen proteins were dysregulated in the tear samples of O-KC groups compared to controls ($P < 0.05$). Dysregulated proteins were associated with oxidative stress, cell adhesion, cytoskeleton organization, and mechanotransduction paths such as RhoA, mTOR, or E-cadherin/N-cadherin signaling. LRA determined three protein panels with high sensitivity-specificity for discriminating between the control and O-KC groups with different biomechanical risks.

Conclusions. This study revealed promising new biomarkers for early detection of KC risk. Oxidative stress and cellular structural alterations seem to begin long before clinical signs and even before the biomechanical alterations can be detected with current clinical tools. Understanding how an initial imbalance of oxidative stress affects cellular mechanobiology is critical to developing new therapeutic strategies for the early treatment of KC.

Keywords: corneal biomechanics, keratoconus offspring, proteomics, tear fluid

Keratoconus (KC) is a chronic and degenerative corneal ectasia that leads to severe visual impairment because of irregular astigmatism and high-order aberrations arising from weakening, thinning, and protrusion of the corneal tissue.[1] KC affects all ethnicities and both sexes, begins in adolescence (or even earlier), and progresses up to 30 to 40 years of age, causing a strong impact throughout the patient's life.[2] KC evolves quickly in its early stages and becomes especially aggressive in its development in children, often reaching considerably more severe stages than when it develops in late adolescence.[3–5] Approximately 28% of children with KC present an already advanced state of the disease at the time of diagnosis.[6] Therefore an early diagnosis and a careful follow-up are crucial to providing adequate management of the disease, because, in advanced stages, KC remains one of the most frequent causes of corneal keratoplasty with limited visual recovery.[7]

Investigative Ophthalmology & Visual Science

Advances in new methods for assessing corneal biomechanics have provided new insights into the alterations at this level in the KC cornea. In this sense, it is considered that the molecular and morphological changes that occur in the corneal tissue cells during KC development modify the focal biomechanical properties of the corneal structure, promoting tissue protrusion and leading to tomographic and topographic alterations.[8,9] This mismatch of biomechanical properties before corneal tissue protrusion has underlined the importance of studying the biomechanical response in early clinical screening for KC, evidencing a paradigm shift for prediction and early diagnosis of corneal ectasias. In this way, the rising popularity of corneal biomechanics examination in recent years has allowed the development of indexes that accurately discriminate the biomechanical alterations that could lead to the onset of corneal ectasias (as is the case of the Corvis Biomechanical Index [CBI; Corvis ST]) when no biomicroscopic or tomographic warning signs are yet evident.[8] However, the molecular alterations leading to such biomechanical instability are still unexplored, opening a promising challenge for understanding early ectasia stages. Although the etiology of KC is still not entirely clear, previous studies have concluded that genetic predisposition and mechanical-environmental factors play an essential role in its development.[10]

The genetic background of KC has long been suggested based on the higher concordance of the disease in monozygotic over dizygotic twins,[11,12] as well as on its association with other genetic syndromes such as Down syndrome,[13,14] Ehlers-Danlos syndrome,[15] or Leber's congenital amaurosis.[16,17] Besides that, a family history of KC is consistently identified as the leading risk factor for the disease development. In this sense, up to 26% of KC patients reported having relatives affected by the disease,[18] and first-degree KC relatives have shown a high prevalence of the disease (15 to 67 times higher risk of disease development) compared to the general population.[19] Moreover, disease progression could be more severe when two or more relatives with KC coexist within the family.[20,21] For these reasons, first-degree pediatric relatives of KC patients are considered the most vulnerable population for disease development.

In the search for KC biomarkers, tear fluid has become an attractive and accessible source that could be useful in identifying the molecular targets responsible for KC development.[22–26] Currently the diagnosis of KC is based on clinical and imaging tools that provide evidence of the signs of manifest disease, but without the ability to predict the predisposition for KC onset and progression. Based on the vulnerability of first-degree pediatric KC relatives to develop the disease, as well as the potential of tear fluid as a biomarker source, the purpose of this study is to analyze quantitatively and qualitatively the tear proteome of young KC offspring using micro–liquid chromatography coupled to tandem mass spectrometry, trying to get closer to the molecular drivers underlying the alterations in corneal biomechanical properties at at-risk stages of KC and to provide new insights into the molecular mechanisms involved in the earlier stages of the disease.

Methods

Study Design and Participants

Study Design. The present study was performed following the principles of the Declaration of Helsinki of the World Medical Association. The Ethics Committee for Clinical Research of Galicia (2019/623) authorized the ophthalmologic clinical protocol and the extraction of biological samples. In terms of study design, this was a cross-sectional study involving a total of 42 eyes from 42 control subjects without a family history of KC and 160 eyes from 80 young offspring of KC patients. All participants underwent an ophthalmological examination with tear fluid extraction. Each participant was informed and asked to sign a consent form outlining the study objectives, ophthalmologic procedures, biological sample collection, and potential undesirable events associated with biological sample extraction. The same researchers performed all the tests. The ophthalmologic protocol included anamnesis, biomechanical and tomographic corneal imaging studies, as well as ocular health examination. Tear fluid was collected using Schirmer strips.

Full anamnesis collected data about age, sex, ocular history, medical history (allergies, asthma, rhinitis, atopic dermatitis, or any condition relevant to the present study), and family history of corneal ectasia or other ocular conditions. A biomechanical scan was performed to determine the corneal dynamic behavior in response to an air-puff pulse. Corvis ST (Oculus, Wetzlar, Germany) was used for the biomechanical assessment. Detailed information on all the Corvis ST parameters studied is available in Supplementary Methods 1. Tomographic imaging was carried out using Pentacam HR (Oculus). The Pentacam HR parameters evaluated are listed in Supplementary Methods 1. Ocular health examination was based on an in-depth biomicroscopic assessment to identify any signs on the ocular surface related to KC disease or other ocular conditions.

Study Subjects. This study involved 122 subjects divided into two groups: 42 control participants without a family history of KC (control group) and 80 young offspring of patients diagnosed with KC (O-KC, study group). All participants were recruited at the Instituto Galego de Oftalmoloxía in Santiago de Compostela, Spain. All participants in this study reported European ancestry. Inclusion criteria for the study group included having a parent diagnosed with clinical KC, supported by slit-lamp examination and corneal topography and tomography examinations. Participants belonging to this group could have corneal features consistent with normal corneal architecture, a subclinical state of KC, or clinical manifestation of the disease. Specifically, the eyes of the O-KC patients were classified according to the CBI biomechanical index. The CBI index results from a logistic regression analysis that considered corneal deformation and stiff parameters together with corneal thickness and pachymetric progression, reaching 100% specificity and 94% sensitivity to identify the KC risk.[8] The CBI ranges from 0 to 1 and determines the risk of ectasia development as follows:[8]

- CBI < 0.25 denotes a low risk of ectasia development.
- CBI 0.25–0.50 denotes a moderate risk of ectasia development.
- CBI > 0.50 denotes a high risk of ectasia development.

In this regard, a total of three study subgroups were determined: (1) eyes of offspring of KC patients with low-risk ectasia development [CBI<0.25] (O-KC-LR group), (2) eyes of offspring of KC patients with moderate risk of ectasia development [CBI 0.25-0.50] (O-KC-MR group), and (3) eyes of offspring of KC patients with a high risk of ectasia development [CBI > 0.50] (O-KC-HR group).

About the control group, the main inclusion criteria were not having any family member diagnosed with subclinical or clinical KC (neither first-degree relatives nor any other relatives), having normal clinical parameters without alterations in the tomographic evaluation, not presenting irregular astigmatism that could suggest a subclinical state of the disease, as well as showing a CBI-index in the biomechanical examination lower than 0.25 (indicative of a low risk of ectasia development).

Common inclusion requirements for all groups were conjunctival hyperemia <2 (Nathan Efron scale[27]), Schirmer test >15 mm in five minutes, and at least five days without contact lenses, artificial tears, or eye drops. Previous surgical intervention in the anterior segment, active ocular or systemic inflammation, current treatment with local or systemic anti-inflammatory drugs, or other corneal or systemic diseases (renal, hepatic, hematologic diseases, or solid tumors) were the exclusion criteria for both groups.

Sample Extraction and Processing

Sample Extraction. The tear samples were extracted by placing a Schirmer strip (Tear Strips; Contacare Ophthalmics & Diagnostics, Gujarat, India) over the lower eyelid about 3 mm from the lateral edge. One strip was used for each eye and was removed when the sample reached 15 mm on the Schirmer scale (9 µL), remaining in contact with the ocular surface for less than five minutes. Tear samples were extracted under suitable environmental conditions and without previous administration of drugs, artificial tears, or vital dyes. Immediately after collection, the strips were frozen and stored at −80°C until their analysis.

Sample Preparation. Firstly, the Schirmer's strips were thawed for 30 minutes at 4°C. For protein extraction, Schirmer strips were cut and incubated for one hour (h) at 4°C in a 100 µL solution of 100 mM ammonium bicarbonate. Samples were spun in a centrifuge for 20 minutes at 13,000*g*, and the supernatant was placed in a new Eppendorf tube. Acetone 600 µL was added to the new Eppendorf tube with the supernatant and incubated at −20°C overnight. Subsequently, samples were spun in a centrifuge for 20 minutes at 13,000*g*, and the supernatant was removed. To evaporate the acetone, the pellet was dried at room temperature (RT) for one hour, and then 100 µL of miliQ water was added. Finally, an RC-DC kit (Bio-Rad Laboratories, Hercules, CA, USA) was used to measure the amount of protein.[28]

Mass Spectrometry Analysis by TripleTOF 6600 LC-MS/MS System

Tryptic Digestion. As for trypsin digestion, 100 µg of protein from the tear fluid of 202 samples (42 controls and 160 O-KC) was loaded on a 10% SDS-PAGE gel. The run was interrupted when the front penetrated 3 mm into the resolving gel.[29,30] The protein band was visualized, with Sypro-Ruby fluorescent staining (Lonza, Porriño, Pontevedra, Spain), excised, and processed for in-gel tryptic digestion as previously described by our group.[25,26] For more details, see Supplementary Methods 2.

Data-Dependent Acquisition (DDA) and Protein Quantification by SWATH-MS (Sequential Window Acquisition for All Theoretical Mass Spectra). Both proteomic analyses, qualitative (DDA) and quantitative (SWATH-MS), were performed as described previously by our group.[25,26] Detailed protocols are available in Supplementary Methods 2. Mass spectrometry proteomics data have been deposited in the ProteomeXchange Consortium via the PRIDE partner repository with the dataset identifier PXD049296.

Protein Interaction Networks and Gene Ontology Analysis

Bioinformatic tools were used to determine the protein-protein interaction networks and to perform the Gene Ontology enrichment analysis (GO). Via the STRING program (free access at https://string-db.org), we created the protein interaction maps. FunRich (Function Enrichment Interaction Analysis) and Shiny GO 0.80 (free access at http://bioinformatics.sdstate.edu/go/) software were used to explore the main biological pathways, molecular functions, and cellular components related to dysregulated proteins. Venn diagram was created with the Bioinformatics &Evolutionary Genomics tool (free access at http://bioinformatics.psb.ugent.be/webtools/Venn/). We used UniProt codes for the search and identification of each protein.

ELISA Validation

Lactoferrin (LF), cofilin-1 (CFL1), and calpain-1 catalytic subunit (CAPN1) expression were measured in human tears using commercial kits of Enzyme-Linked Immunosorbent Assays (ELISA) from FineTests [LF (ELISA kit catalog number EH0396); CFL1 (ELISA kit catalog number EH1788); CAPN1 (ELISA kit catalog number EH2761)]. All assays were carried out following the manufacturer's protocols and were optimized and used with the following dilution factors: 1:100000 for LF, 1:50 for CFL1, and 1:5 for CAPN1. Tear samples were assayed in duplicate, and mean expression values were reported as ng/mL. Curve Expert 1.4 and Microsoft Excel were used for curve and data analysis, and graphs were performed using GraphPad Prism 8.0 (San Diego, CA, USA).

Construction of the Regression Model

Proteins with the highest discriminatory power for the detection of corneal biomechanical changes and KC-risk were analyzed using logistic regression (LRA) to develop the simplest predictive models for each condition. For model fitting and coefficient estimation, we applied a backward method using Akaike's information criterion as a global selection criterion. Considering the following logit formula, those proteins that achieved LRA statistical significance were selected and gathered to define the different protein panels:

$$\pi\,(x_1, x_2 \ldots, x_n) = \frac{e^{x'\beta}}{1 + e^{x'\beta}}$$

$$^{*}x'\beta = \beta_0 + \beta_1 x_1 + \beta_2 x_2 \ldots + \beta_n x_n.$$

Statistical Analysis

GraphPad Prism 8.0 and R 4.3.3 software were used for statistical analysis. Categorical variables were represented as percentages. Continuous quantitative variables with a normal distribution were expressed with the mean (±SD), and variables with a non-normal distribution were presented as median [interquartile range]. D'Agostino test was performed to confirm the normality of the quantita-

tive variables. Bivariate comparisons were performed using the chi-square test (for categorical variables), and parametric (Student *t*) or nonparametric (Mann-Whitney U/ Kruskal-Wallis) test for continuous variables according to their normality. $P \leq 0.05$ value was considered statistically significant in all tests. Fold change (FC) was calculated as the ratio of the difference between the protein expression (expressed as normalized area) in each group analyzed. FC indicates upregulation if FC > 1 or downregulation if FC < 1. Dysregulated proteins were analyzed by LRA, fitted using a backward elimination method and Akaike's information criterion as a global selection criterion to identify the optimal subset of predictors to model the probability of the different biomechanical conditions. Receiver operating characteristic (ROC) curve analysis was performed using the pROC R package to determine the potential role of combining dysregulated proteins as biomarkers for discriminating alterations in corneal biomechanical properties and detecting the risk associated with having a parent diagnosed with KC. Cutoff values were selected looking for a good balance between sensitivity and specificity.

Results

Clinical Features

In this study, we included 42 healthy eyes from 42 control subjects (61.1% male; mean age, 13.15 ± 4.87 years) and 160 eyes from 80 offspring of KC patients (O-KC, 55.4% male; mean age, 12.31 ± 3.30 years). Focusing on corneal biomechanical alterations, O-KC eyes were classified into three risk groups for ectasia development according to the CBI index. Based on this, a total of 42 eyes were included in the control group, 114 eyes in the O-KC-LR group [CBI < 0.25], 28 eyes in the O-KC-MR group [CBI 0.25-0.50], and 18 eyes in the O-KC-HR group [CBI > 0.50]. Table 1 shows the analysis of demographic (age, sex) and clinical data associated with KC (presence of allergic disease, ocular itching, and eye rubbing) between controls and O-KC groups.

No differences were observed for sex, history of allergic disease, eye itching, or ocular rubbing between groups. No significant age differences were found between groups except for the moderate- and high-risk groups, which showed higher ages than the low-risk group.

About biomechanical metrics, Table 2 shows the comparisons of the Corvis ST parameters between the control and study groups. No differences were observed between the control and the O-KC-LR group. As expected, the main statistical differences were observed in the O-KC-MR and O-KC-HR groups compared to the remaining ones, concerning the stiffness data (SP-A1), the viscoelastic properties (DARatio max [1 mm], DARatio max [2 mm], and IR), as well as the parameters of corneal pachymetry and pachymetric progression (CCT_C, ARTh and Pachy Slope). In comparison to the control and O-KC-LR groups, both O-KC-MR and O-KC-HR showed lower SP-A1 (indicating a decrease in the stiffness of the corneal tissue), differences in central pachymetry and pachymetric progression (evidencing lower corneal thickness and alterations in corneal thickness progression), and an increase in the values of the DARatio max and IR (pointing out an increase in the central corneal deformation amplitude).

Regarding corneal tomography, Table 3 presents the tomographic data and the comparisons between groups. No differences were observed between the control and the O-KC-LR group. The O-KC-MR group showed significant differences in pachymetry and pachymetric progression parameters (CCT_P, MTP, and ARTmax) and KC indexes (BAD-D, TBI), in comparison to the control group ($P = 0.001$, $P = 0.001$, $P = 0.015$, and $P = 0.040$, $P = 0.001$; respectively) and the O-KC-LR group ($P = 0.001$, $P = 0.001$, $P = 0.003$, and $P = 0.028$, $P = 0.001$; respectively), evidencing a decrease in the corneal thickness and higher values for the KC tomographical detection indexes. Predictably, O-KC-HR showed significant differences in all the parameters studied compared to the control and O-KC-LR groups. When comparing the O-KC-MR and O-KC-HR groups, there were no differences in terms of pachymetry; however, all other parameters evaluated (including corneal curvature, asymmetry, anterior and posterior corneal elevation, and KC indexes) were significantly higher in the O-KC-HR group ($P = 0.001$).

Assessment of Tear Proteomics Based on Biomechanical Screening

SWATH-MS results were analyzed to identify the differential proteins between the control and O-KC groups, as well as target proteins associated with corneal biomechanical alterations. In this way, we observed the dysregulation of 15 proteins in the tear fluid of O-KC groups, including the under expression of Lipocalin-1 (LCN-1), Lactoferrin (LF), Argininosuccinate synthase (ASS1), Cofilin-1 (CFL1), Calpain-1

Table 1. Analysis of Demographics and Clinical Variables of Controls and O-KC Groups

Variable	Control	O-KC-LR	P*	O-KC-MR	P†	O-KC-HR	P‡	P§	P‖	P¶
Age (years)	13 ± 4.8	10 ± 3	0.106	13 ± 2.5	0.248	16 ± 3.7	0.070	**0.010**	**0.002**	0.348
Sex (% male)	61.0	54.2	0.656	53.3	0.757	66.7	1.000	1.000	0.707	0.678
Allergic disease (%)	14.7	18.2	0.774	30.0	0.159	30.0	0.355	0.212	0.417	1.000
Ocular itching (%)	14.5	24.5	0.165	24.0	0.350	18.8	0.703	0.958	0.759	1.000
Eye rubbing (%)	12.9	24.5	0.107	20.0	0.687	18.8	0.687	0.795	0.759	1.000

Sample size: Control (control group, $n = 42$ eyes, 42 control subjects), O-KC-LR (eyes of offspring of KC patients with low risk of ectasia development, $n = 114$ eyes, 59 offspring of KC patients), O-KC-MR (eyes of offspring of KC patients with moderate risk of ectasia development, $n = 28$ eyes, 19 offspring of KC patients), O-KC-HR (eyes of offspring of KC patients with a high risk of ectasia development, $n = 18$ eyes, 10 offspring of KC patients). *P*-values in bold show statistically significant comparisons.

* O-KC-LR compared to control.
† O-KC-MR compared to control.
‡ O-KC-HR compared to control.
§ O-KC-LR compared to O-KC-MR.
‖ O-KC-LR compared to O-KC-HR.
¶ O-KC MR compared to O-KC-HR.

Investigative Ophthalmology & Visual Science

Table 2. Analysis of Corvis ST Biomechanical Parameters in Control and O-KC Groups

Parameters	Control	O-KC-LR	P^*	O-KC-MR	$P^\dagger$	O-KC-HR	$P^\ddagger$	$P^\S$	$P^\|$	$P^\P$
bIOP (mm Hg)	15.60 ± 2.04	16.24 ± 1.88	0.096	15.84 ± 2.20	0.933	15.15 ± 1.90	0.223	0.364	0.053	0.290
A1T (ms)	7.37 ± 0.29	7.44 ± 0.25	1.000	7.24 ± 0.24	0.504	7.18 ± 0.22	0.189	**0.005**	**0.003**	1.000
A1V (m/s)	0.14 ± 0.01	0.14 ± 0.01	1.000	0.15 ± 0.02	1.000	0.16 ± 0.02	0.652	0.711	**0.049**	1.000
A2T (ms)	22.15 ± 0.40	22.01 ± 0.32	0.813	22.20 ± 0.47	1.000	22.14 ± 0.30	1.000	0.205	1.000	1.000
A2V (m/s)	−0.27 ± 0.03	−0.25 ± 0.06	0.992	−0.27 ± 0.03	1.000	−0.28 ± 0.03	1.000	1.000	0.470	1.000
HCT (ms)	17.29 ± 0.67	17.29 ± 0.52	1.000	17.44 ± 0.52	1.000	17.25 ± 0.54	1.000	1.000	1.000	1.000
DAmax (mm)	1.12 ± 0.10	1.06 ± 0.09	**0.048**	1.12 ± 0.10	1.000	1.15 ± 0.09	1.000	**0.041**	**0.006**	1.000
HCDA (mm)	0.91 ± 0.10	0.86 ± 0.09	0.169	0.91 ± 0.09	1.000	0.97 ± 0.10	0.334	0.064	**0.001**	0.643
A1DLL (mm)	2.38 ± 0.11	2.36 ± 0.16	1.000	2.32 ± 0.12	0.251	2.32 ± 1.14	1.000	0.504	1.000	1.000
A2DLL (mm)	3.33 ± 0.65	3.21 ± 0.67	1.000	3.01 ± 0.86	1.000	2.85 ± 0.83	0.350	1.000	0.659	1.000
HCDLL (mm)	6.68 ± 0.50	6.43 ± 0.40	0.054	6.57 ± 0.27	1.000	6.61 ± 0.43	1.000	1.000	1.000	1.000
PD (mm)	5.06 ± 0.27	4.92 ± 0.27	0.155	5.09 ± 0.19	1.000	5.11 ± 0.26	1.000	**0.035**	0.059	1.000
DARatio max (1 mm)	1.52 ± 0.05	1.52 ± 0.05	0.685	1.55 ± 0.04	**0.039**	1.58 ± 0.05	0.000	**0.004**	**0.000**	0.073
DARatio max (2 mm)	4.04 ± 0.36	4.06 ± 0.32	0.885	4.36 ± 0.30	**0.013**	4.76 ± 0.52	0.000	**0.002**	**0.000**	**0.004**
IR [mm^{-1}]	7.87 ± 1.06	7.79 ± 0.87	0.657	8.43 ± 0.82	0.294	9.37 ± 1.27	0.000	**0.022**	**0.000**	**0.018**
MaxInverseRadius (mm^{-1})	0.165 ± 0.02	0.162 ± 0.06	0.783	0.173 ± 0.01	0.515	0.188 ± 0.02	0.133	0.285	0.052	0.348
CCT_C (µm)	550 ± 27	549 ± 33	1.000	519 ± 24	**0.001**	509 ± 30	**0.001**	**0.001**	**0.001**	1.000
ARTh	691 ± 194	685 ± 161	0.860	529 ± 137	**0.002**	418 ± 108	**0.000**	**0.000**	**0.000**	0.276
Pachy Slope (µm)	34 ± 10	34 ± 8	0.963	38 ± 7	0.791	44 ± 12	**0.000**	0.355	**0.000**	0.152
SP-A1	99 ± 14	100 ± 12	0.578	87 ± 13	**0.007**	81 ± 13	**0.000**	**0.000**	**0.000**	1.000
CBI	0.12 ± 0.09	0.17 ± 0.14	1.000	0.50 ± 0.10	**0.001**	0.75 ± 0.22	**0.001**	0.001	**0.001**	**0.001**
SSI	0.91 ± 0.14	0.99 ± 0.15	0.205	0.96 ± 0.14	1.000	0.83 ± 0.15	0.671	1.000	**0.000**	0.062

Sample size: Control, control group ($n = 42$ eyes), O-KC-LR, eyes of offspring of KC patients with low risk of ectasia development ($n = 114$ eyes); O-KC-MR, eyes of offspring of KC patients with moderate risk of ectasia development ($n = 28$ eyes); O-KC-HR, eyes of offspring of KC patients with a high risk of ectasia development ($n = 18$ eyes).

Parameters: bIOP, biomechanical corrected intraocular pressure; A1T/A2T, first/second applanation time; A1V/A2V, first/second applanation velocity; HCT, time to the highest concavity; DAmax, deformation amplitude; HCDA, deflection amplitude at highest corneal concavity; A1DLL/A2DLL, first/second applanation deflection length; HCDLL, highest concavity deflection length; PD, peak distance at the highest concavity; DAratio max 1 mm, maximum deformation amplitude ratio at 1 mm; DAratio max 2 mm, deformation amplitude ratio max 2 mm; IR, integrated radius; Max Inverse Radius, maximum inverse radius; CCT_C, central corneal thickness by Corvis; ARTh, Ambrósio Relational Thickness horizontal; Pachy Slope, changes of corneal thickness from the corneal center to the periphery; SP-A1, CBI, and SSI (stress-strain index). *P*-values in bold show statistically significant comparisons.

[*] O-KC-LR compared to control.
[†] O-KC-MR compared to control.
[‡] O-KC-HR compared to control.
[§] O-KC-LR compared to O-KC-MR.
[‖] O-KC-LR compared to O-KC-HR.
[¶] O-KC MR compared to O-KC-HR.

catalytic subunit (CAPN1), Superoxide Dismutase (SOD1), Ezrin (EZR), Peroxiredoxin-1 (PRDX1), Hemopexin (HPX), α-actinin 4 (ACTN4), and Actin cytoplasmic 2 (ACTG); and the overexpression of Keratin type II cytoskeletal 5 (KRT5), Apolipoprotein A-I (APOA1), Protein S100 A11 (S100A11), and Apolipoprotein A-II (APOA2). Supplementary Results 1 includes the statistical data of the comparative analysis among groups of the 15 dysregulated proteins. Figure 1 shows, as volcano plots and heatmaps, the 15 dysregulated proteins in the O-KC tear samples. The FC values indicate the ratio of under- or overexpression of each protein.

Most of these proteins showed differential expression in all groups of O-KC compared to the control, even in those cases without detectable alterations in corneal biomechanical properties (O-KC-LR). In general, as biomechanical indexes revealed an increased risk of developing corneal ectasia, the expression of these proteins maintained a trend toward their under- and overexpression. Figure 2 represents the median [interquartile range] of the MLR-normalized SWATH-MS area of each dysregulated protein.

LCN-1, LF, and SOD1 were the most underexpressed proteins in O-KC samples, showing their lower expression in the O-KC-MR and O-KC-HR groups. ASS1 was underexpressed in the O-KC-LR and O-KC-MR groups compared to controls; however, no significant differences in its expression were observed among the O-KC groups. Subsequently, CFL1, CAPN1, EZN, PRDX1, and HPX had lower expression in all O-KC groups compared to controls, and ACTN4 and ACTG, two proteins belonging to the actin family, showed their minimum expression in O-KC-MR.

Regarding overexpressed proteins, statistical analysis revealed that KRT5 substantially increased its expression in the O-KC-HR group, remaining similar to control levels in the low-risk and moderate-risk groups. APOA1 was up-regulated in all O-KC groups, but the increase was statistically significant only for O-KC-LR and O-KC-MR groups compared to controls. Finally, S100A11 and APOA2 were the two proteins with the highest expression in the O-KC groups compared to controls, and this significant overexpression was stable in all the groups independently of the differences in the biomechanical response. Correlation analysis was performed to assess the influence of age on the dysregulated proteins. As a result, no relationship was observed between any dysregulated protein and the age factor ($P > 0.05$ in all study correlations, Supplementary Results 1). As for functional implications of dysregulated proteins, Figure 3 shows the main biological processes, molecular functions, and cellular components related to the down- and up-regulated proteins in O-KC groups.

Table 3. Analysis of Pentacam HR Tomographic Parameters in Control and O-KC Groups

Parameters	Control	O-KC-LR	P^{*}	O-KC-MR	$P^{\dagger}$	O-KC-HR	$P^{\ddagger}$	$P^{\S}$	$P^{\|}$	$P^{\P}$
PDC (D)	42.78 ± 1.27	43.28 ± 1.22	0.187	43.01 ± 1.28	0.645	45.97 ± 5.52	**0.001**	0.537	**0.001**	**0.001**
K1 (D)	42.23 ± 1.27	42.70 ± 1.24	0.089	42.34 ± 1.25	0.768	44.13 ± 2.75	**0.001**	0.252	**0.001**	**0.001**
K2 (D)	43.34 ± 1.24	43.57 ± 1.52	0.444	43.39 ± 1.32	0.909	46.00 ± 3.46	**0.001**	0.591	**0.001**	**0.001**
Kmax (D)	43.89 ± 1.36	44.12 ± 1.26	0.522	43.99 ± 1.50	0.802	48.79 ± 6.76	**0.001**	0.790	**0.001**	**0.001**
I-S asymmetry (D)	−0.25 ± 0.60	−0.05 ± 0.57	0.274	0.07 ± 0.87	0.193	1.42 ± 2.69	**0.001**	0.562	**0.001**	**0.001**
ARTmax (µm)	459 ± 69	455 ± 91	0.916	401 ± 68	**0.015**	287 ± 79	**0.001**	**0.003**	**0.001**	**0.001**
CCT_P (µm)	546 ± 26	549 ± 33	0.637	519 ± 25	**0.001**	510 ± 30	**0.001**	**0.001**	**0.001**	0.301
MTP (µm)	542 ± 24	546 ± 32	0.550	516 ± 24	**0.001**	504 ± 30	**0.001**	**0.001**	**0.001**	0.191
AE (µm)	3.00 (2.00)	3.00 (2.00)	0.685	3.00 (3.00)	0.791	4.50 (7.00)	**0.001**	0.965	**0.001**	**0.001**
PE (µm)	6.00 (6.25)	6.50 (8.00)	0.461	7.00 (11.00)	0.659	11.00 (29.75)	**0.001**	0.898	**0.001**	**0.001**
BAD-D	0.75 (0.56)	0.75 (0.84)	0.800	1.31 (0.90)	**0.040**	1.94 (1.96)	**0.001**	**0.028**	**0.001**	**0.001**
TBI	0.00 (0.12)	0.08 (0.18)	0.169	0.20 (0.47)	**0.001**	0.65 (0.85)	**0.001**	**0.001**	**0.001**	**0.001**

Sample size: Control, control group (n = 42 eyes); O-KC-LR, eyes of offspring of KC patients with low risk of ectasia development (n = 114 eyes); O-KC-MR, eyes of offspring of KC patients with moderate risk of ectasia development (n = 28 eyes); O-KC-HR, eyes of offspring of KC patients with a high risk of ectasia development (n = 18 eyes).

Parameters: PDC, corneal central power; K1, keratometry in the flattest meridian; K2, keratometry in the steeper meridian; Kmax, maximum dioptric power; I-S asymmetry, inferior-superior dioptric asymmetry; ARTmax, maximum Ambrósio Relational Thickness; CCT_P, central corneal thickness by Pentacam; MTP, minimum thickness point; AE/PE, anterior and posterior surfaces elevation; BAD-D, total deviation value; TBI, Tomographic and Biomechanical Index. *P*-values in bold show statistically significant comparisons.

[*] O-KC-LR compared to control.
[†] O-KC-MR compared to control.
[‡] O-KC-HR compared to control.
[§] O-KC-LR compared to O-KC-MR.
[‖] O-KC-LR compared to O-KC-HR.
[¶] O-KC MR compared to O-KC-HR.

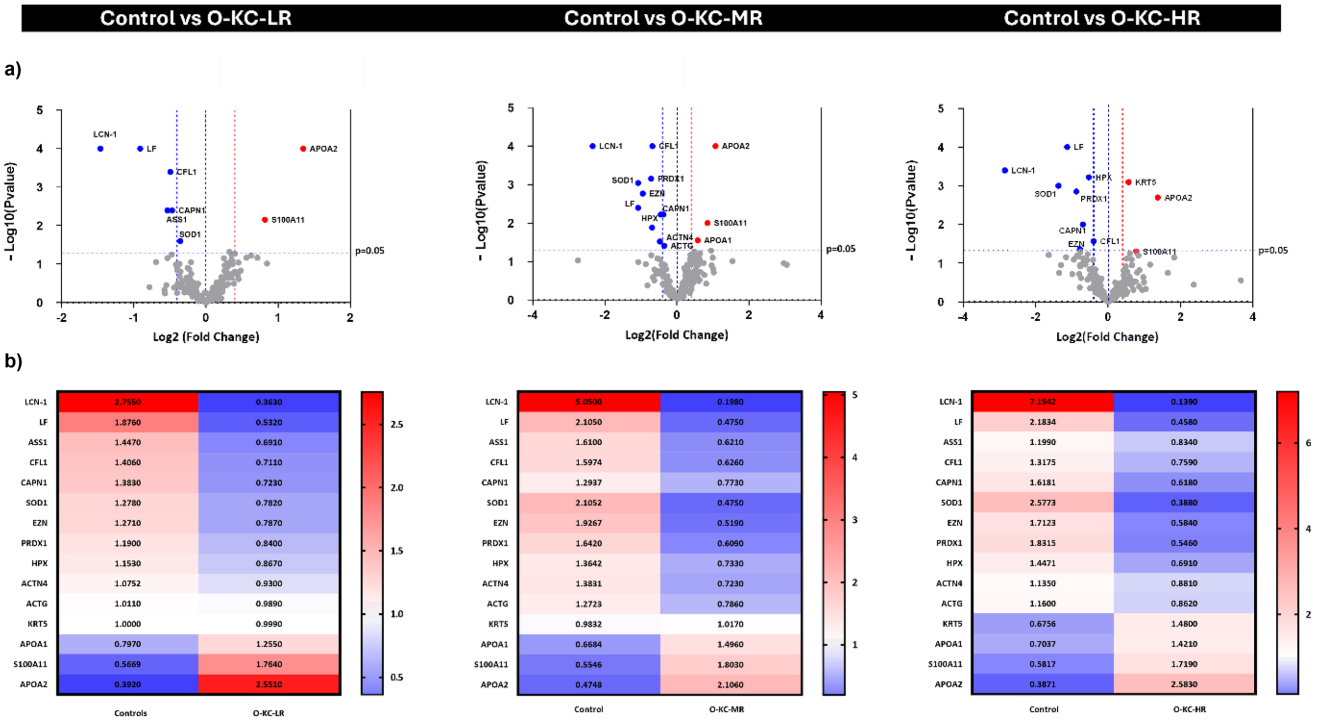

Figure 1. (**a**) Volcano plots represent quantitative proteomics data. Proteins are ranked in a volcano plot according to their statistical *P* value (y-axis) as −log10 and their relative abundance ratio (log2 FC) between the different O-KC groups and control samples (x-axis). Off-centered spots are those that differ the most between the groups. The cutoffs for significant changes are FC of 1.3 and $P < 0.05$. *Blue spots* show the downregulated proteins and *red spots* the upregulated proteins in the specific O-KC group regarding the control. (**b**) Heatmaps represent the fold change of the dysregulated proteins in the study groups compared to the control.

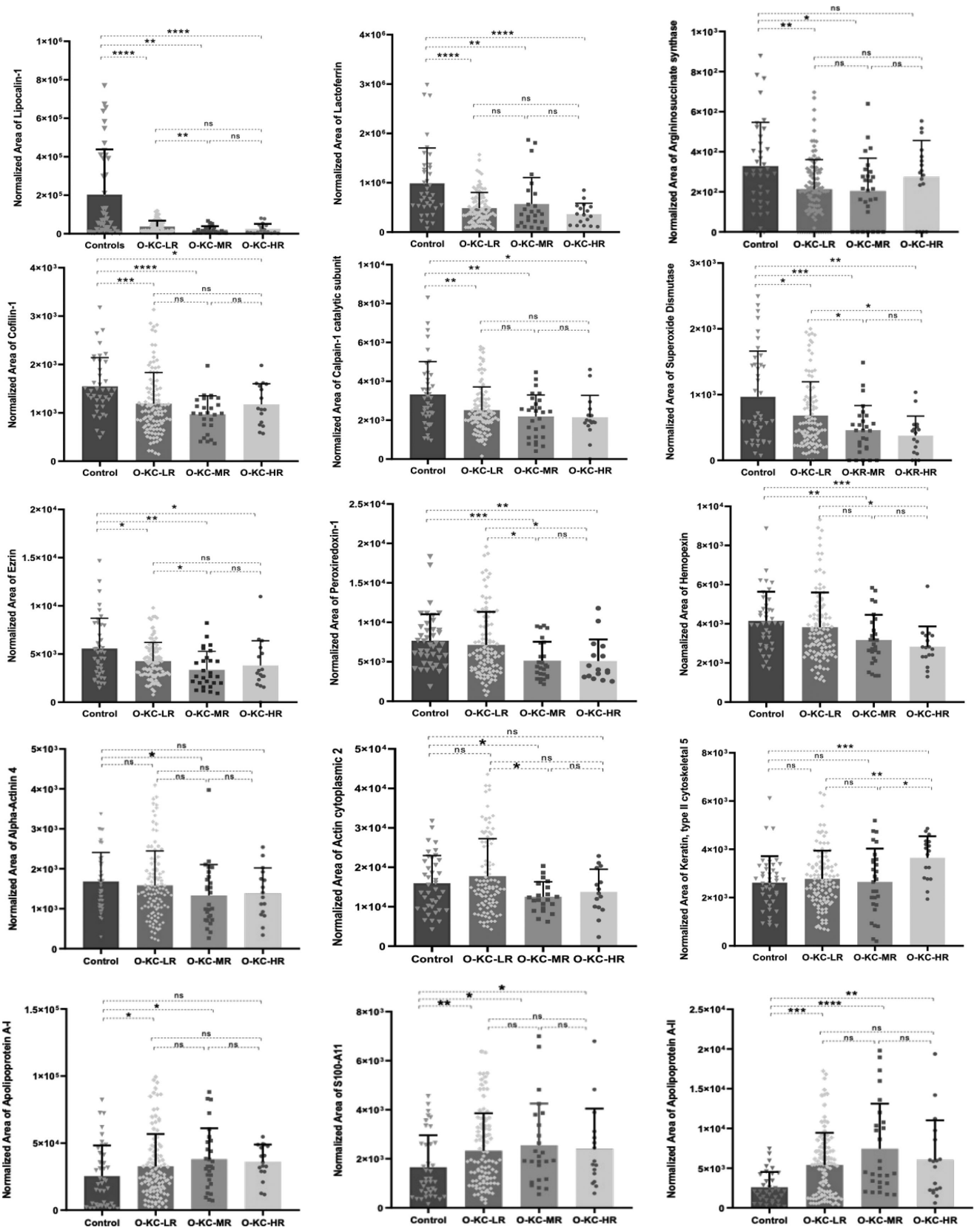

Figure 2. Representation of the median [interquartile range] MLR-normalized SWATH-MS area of the 15 dysregulated proteins in the tear samples of O-KC groups. The normalized area was obtained from the SWATH method for each sample. Sample size: Control (control group, $n = 42$ eyes), O-KC-LR (eyes of offspring of KC patients with low risk of ectasia development, $n = 114$ eyes), O-KC-MR (eyes of offspring of KC patients with moderate risk of ectasia development, $n = 28$ eyes), O-KC-HR (eyes of offspring of KC patients with a high risk of ectasia development, $n = 18$ eyes). *$P < 0.05$, **$P < 0.01$, ***$P < 0.001$, ****$P < 0.0001$, ns: nonsignificant.

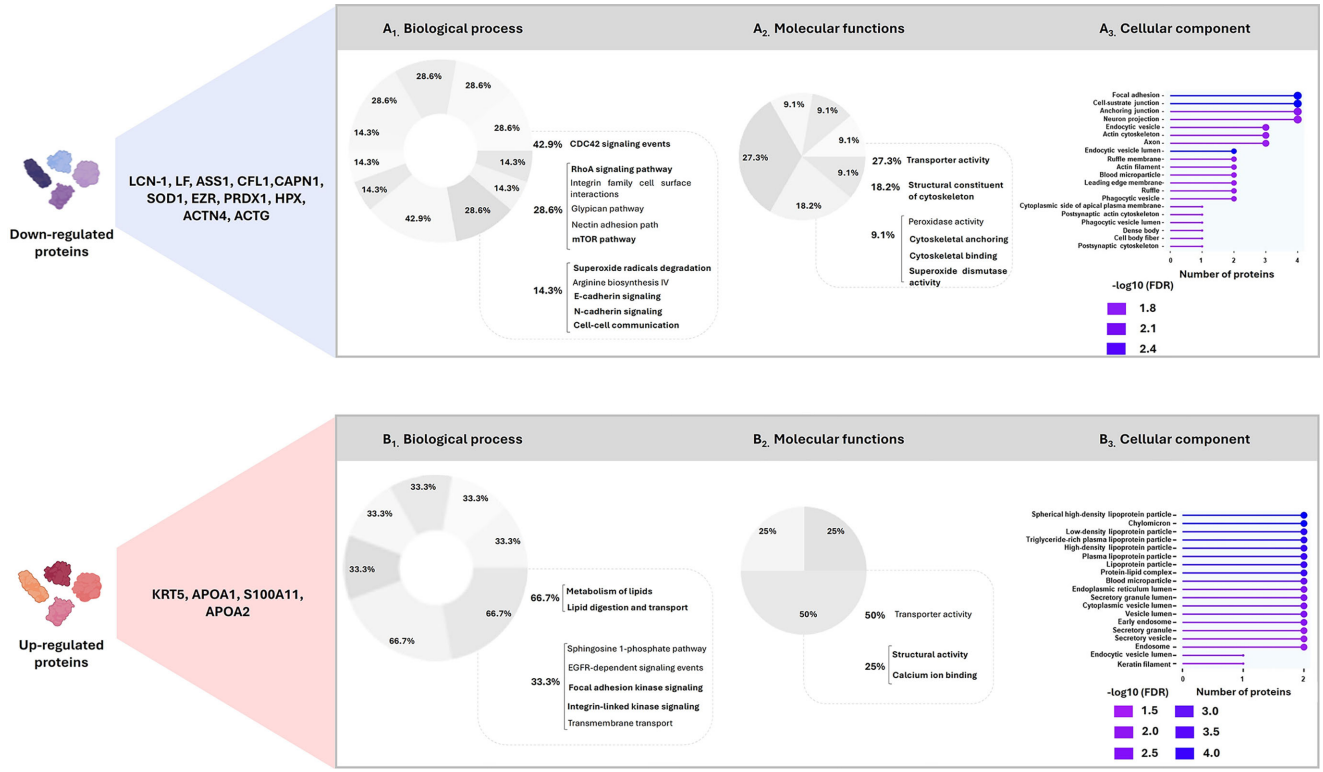

Figure 3. Main biological processes, molecular functions, and cellular components related to the down-regulated ($\mathbf{A_1}$, $\mathbf{A_2}$, $\mathbf{A_3}$) and up-regulated ($\mathbf{B_1}$, $\mathbf{B_2}$, $\mathbf{B_3}$) proteins in the O-KC groups. GO enrichment of dysregulated proteins was made using the FunRich functional tool. Charts represent the main biological processes and molecular functions in which differentially expressed proteins were involved ($P < 0.05$). The percentage of the $\mathbf{A_1}$, $\mathbf{A_2}$, and $\mathbf{B_1}$, $\mathbf{B_2}$ refers to the number of dysregulated proteins involved in this process compared with the total proteins in the database.

Down-regulation of several proteins essential for oxidative protection (LCN-1, LF, SOD1), as well as for cell morphology and migration, cell/cell adhesion, F-actin crosslinking, and actin cytoskeletal organization (CFL1, CAPN1, EZN, ACTN4, and ACTG), underlined the possible impact on paths such as ROS degradation, CDC42 signaling events, focal adhesion kinase signaling events, E-cadherin and N-cadherin signaling paths, and RhoA or mTOR pathways (Fig. 3A_1). In this way, a high percentage of these proteins were related to structural activities at the cytoskeleton level (Fig. 3A_2); and the cellular component analysis showed their membership to focal adhesions, cell/substrate junctions, anchoring junctions, and the actin cytoskeleton (Fig. 3A_3).

Regarding overexpressed proteins (Figs. 3B_1, B_2, and B_3), up-regulation of APOA1 and APOA2 emphasized the enrichment of lipidic processes such as lipoprotein metabolism or lipid digestion, mobilization, and transport. In the same way, the main anatomical entities of the up-regulated proteins were related to lipidic and lipoprotein particles and complexes. Additionally, the overexpression of S100A11 was associated with the enhancement of structural processes such as integrin-linked kinase signaling.

Data-Dependent Workflow Analysis of the Complete Tear Proteome of Control and O-KC Groups

Following a DDA mode, we analyzed the tear proteome of the control and O-KC groups to have a global view of each group's complete tear proteomic profile. This approach enabled the identification of proteins specifically expressed in each group.

With an FDR of less than 10%, 574 proteins were identified in controls, 628 in O-KC-LR, 523 in O-KC-MR, and 396 in O-KC-HR. Figure 4 includes a Venn diagram (a) representing the distribution of unique and overlapping proteins identified in the qualitative analysis of the tear samples of control and O-KC eyes. As a result, out of the total number of proteins identified, 41 were exclusively found in the control group, 49 were only identified in the O-KC-LR group, 20 were uniquely expressed in the O-KC-MR group, and 12 were only in the O-KC-HR group. To determine the potential relevance of these proteins in KC risk and their impact on corneal biomechanical alteration, the biological processes and molecular functions of the proteins linked to each O-KC group were analyzed by the FunRich software (Fig. 4b).

GO analysis targeted at the proteins exclusively identified in each O-KC group revealed the enrichment of pathways with analogous or complementary purposes in all groups. Most of them were related to cell adhesion events through several molecules such as Nectin, E-cadherin, or β-integrin. Similarly, other paths associated with cytoskeletal remodeling, different phases of the cell cycle, and cell aging (cell growth, differentiation, division, migration, or cell death) were also enriched, such as RhoA and mTOR pathways or the CDC42 signaling events, supporting the findings previously observed in the dysregulated proteins of the SWATH-MS analysis.

Moreover, most of the proteins involved in immunity cascades, such as the MyD88 cascade, were only found in

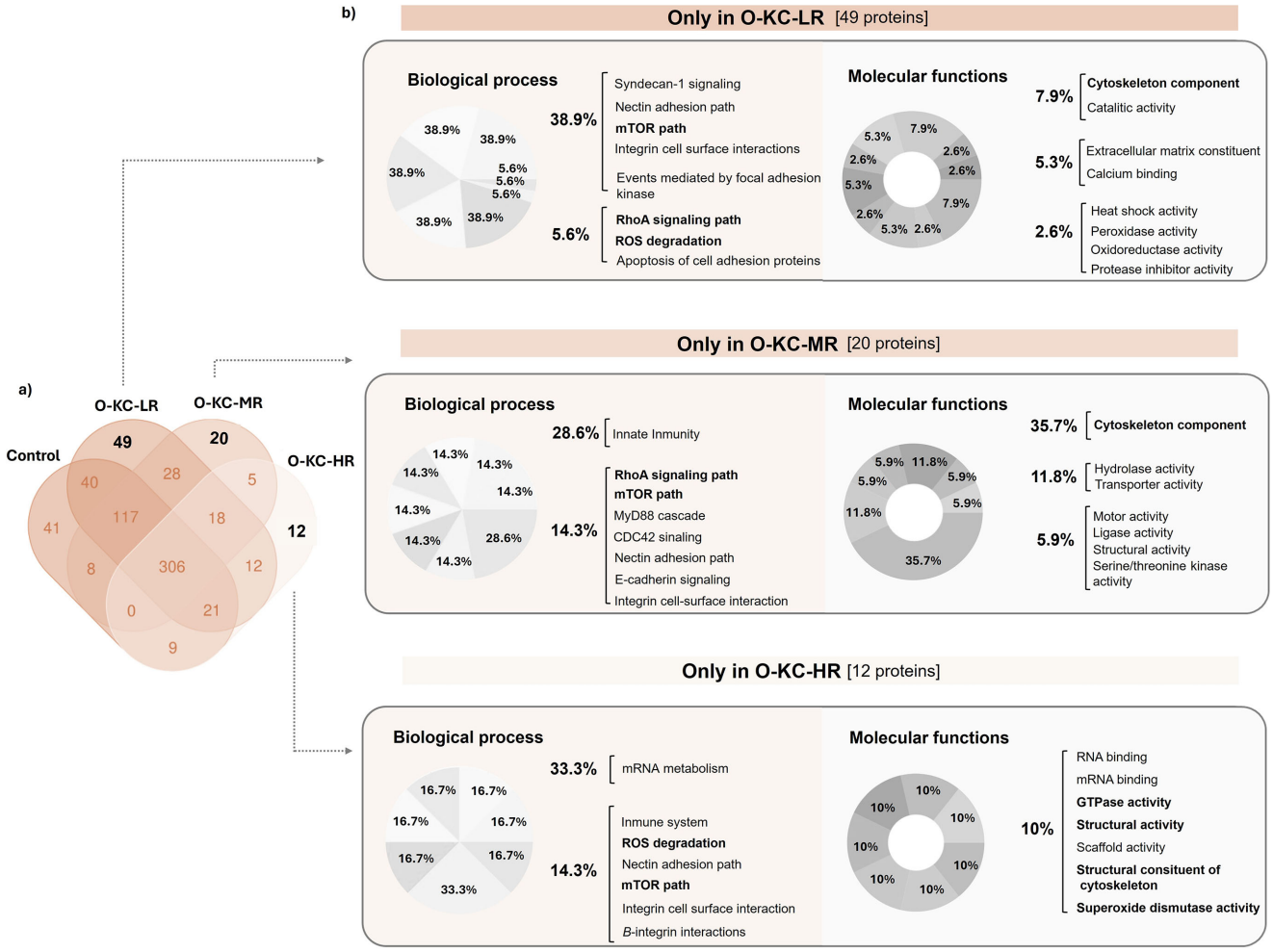

Figure 4. (**a**) Venn diagram represents the distribution of the unique and overlapping proteins identified in the qualitative analysis of the tear samples of control and O-KC eyes. (**b**) Analysis of the biological processes and molecular functions associated with the proteins uniquely identified in the O-KC-LR, O-KC-MR, and O-KC-HR groups. The percentages of the charts refer to the number of proteins involved in these processes compared with the total proteins in the database.

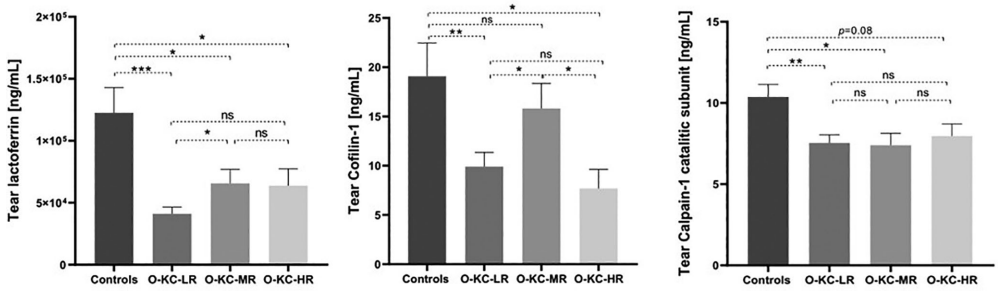

Figure 5. Representation of LF, CFL1, and CAPN1 expression (mean ± SD, ng/mL) in the tear samples of control, O-KC-LR, O-KC-MR, and O-KC-HR eyes, quantified by ELISA. *$P < 0.05$, **$P < 0.01$, ***$P < 0.001$, ns: nonsignificant.

the O-KC-MR and O-KC-HR groups. Regarding the molecular functions, structural activity proteins represented the highest percentage in all O-KC groups.

ELISA Validation

Three proteins were selected for further validation by ELISA based on the results obtained in the LC-MS/MS analysis, as well as the potential molecular involvement of these proteins. ELISA assays confirmed the previously observed findings, revealing LF underexpression in all O-KC groups, lower CFL1 expression in the O-KC-LR and O-KC-HR groups, and reduced CAPN1 levels in all groups of offspring of KC patients. Figure 5 depicts the ELISA quantification of the three proteins for each study group.

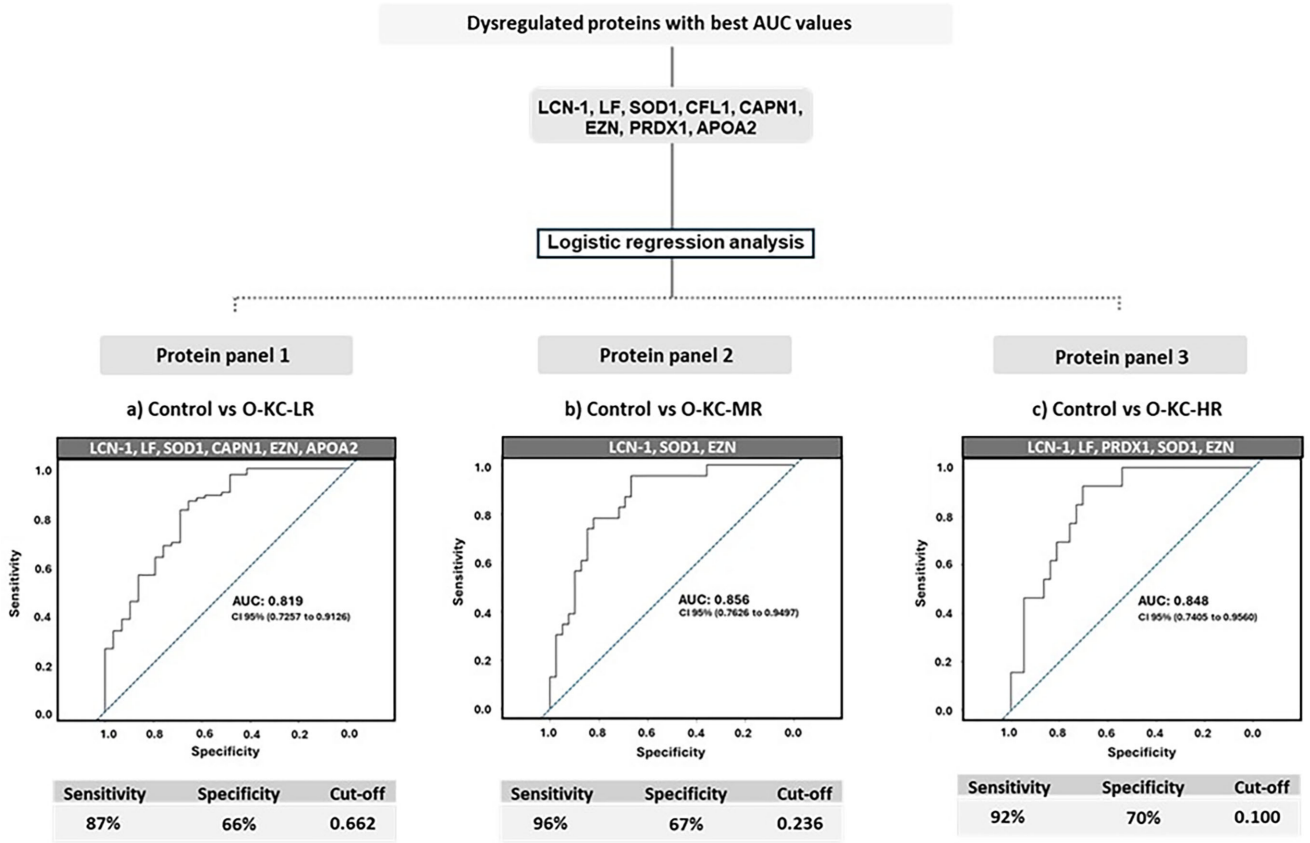

Figure 6. Flowchart representing the LRA and ROC analysis of the three protein panels. (**a**) ROC curve of the regression model including LCN-1, LF, SOD1, CAPN1, EZN, and APOA2 proteins for the O-KC-LR condition. (**b**) ROC curve of the regression model including the protein panel of LCN-1, SOD1, and EZN for the O-KC-MR condition. (**c**) ROC curve of the regression model including LF, LCN-1, PRDX1, SOD1, and EZN for the O-KC-HR condition.

Diagnostic Potential of the Dysregulated Proteins by ROC Analysis and LRA Modeling

ROC of each dysregulated protein in tear samples of O-KC was conducted to predict their ability to discriminate alterations in the corneal biomechanical properties, as well as the risk associated with having a parent with KC. According to the ROC analysis results, LCN-1, LF, SOD1, CFL1, CAPN1, EZN, PRDX1, and APOA2 were the most useful markers to distinguish between controls and O-KC groups. Among them, the highest sensitivity and specificity were found for LCN-1, LF, SOD1, CFL1, CAPN1, and APOA2. The ROC analysis of each protein is given in Supplementary Results 2. LRA was performed to determine the best panels of proteins that significantly influenced each biomechanical condition, defining three models that discriminated with high accuracy the study groups from the control. Figure 6 shows a flow chart describing and summarizing the proteins included in the estimation model for each O-KC group, as well as the AUC, CI, sensitivity, specificity, and cutoff values of each prediction model. Supplementary Results 2 includes details regarding the regression formulas and the breakdown of the ROC analysis for each protein panel.

Discussion

Although family history is considered a significant risk factor for KC,[31] studies exploring the molecular basis underlying KC relatives' susceptibility remain limited and focus primarily on clinical features. Previous studies consistently show that KC relatives often present steeper and thinner corneas, sometimes resembling subclinical KC stages.[32–34] In the same way, biomechanical weakness resulting from decreased corneal stiffness and strength has also been described in KC relatives.[35] From a molecular perspective, first-degree relatives of KC patients showed increased expression of inflammatory and innate immune molecules in tears and corneal/conjunctival epithelial cells.[36,37] In the same way, KC familial genetic studies reported variants in some genes, proposing a likely oligogenic causality in which multiple pathogenic variants reside in an individual within a high-susceptibility genome.[38]

The growing interest in studying corneal biomechanical properties to identify early tissue instability in corneal ectasias has received significant attention in clinical research settings;[39,40] however, no studies to date have explored the protein drivers of these mechanical alterations. In this sense, this study aimed to determine the proteomic alterations in tear fluid associated with both corneal biomechanical properties and the risk of KC development (related to the presence of a parent diagnosed with the disease).

Accordingly, the first step of this study involved assessing the corneal biomechanics of the O-KC eyes. In this way, the biomechanical exploration of the KC offspring group showed that 18% of the eyes had moderate alterations in the corneal dynamics, indicating a moderate risk of ecta-

sia development (O-KC-MR group), and 11% had high alterations in the biomechanical exam, pointing out a high-risk of ectasia development (O-KC-HR). These results align with previous studies, which suggested that first-degree relatives of KC patients could exhibit lower hysteresis and corneal resistance compared to the broader population.[35,41] Additionally, the morphology of the corneal tissue was studied using tomographic imaging, and the most remarkable aspect of the tomographic evaluation was the role of pachymetry metrics. Specifically, central and minimum corneal thickness and pachymetric progression indexes (ARTmax/ARTh) differentiated the moderate and high-risk groups from the remaining ones. Pachymetric defects are well documented in corneal ectasias, with progressive thinning of the ectasic area with severity.[1] Previous studies have reported that KC corneas exhibit significantly weaker biomechanical properties than healthy corneas of equivalent thinning (corneal thinnest point <500 µm).[42] Regarding the spatial corneal thickness, abnormal pachymetric distribution has been reported in KC patients' contralateral eyes, biomechanically and tomographically healthy.[43–45] These findings are consistent with our results, suggesting that slight variations in corneal thickness and pachymetric progression could stimulate/exacerbate alterations in corneal mechanical behavior.

Although the molecular basis of KC are not fully understood, previous studies reveal a key imbalance in its pathophysiology, including increased levels of metalloproteases and the reduced expression of their inhibitors,[22,46,47] increased oxidative stress markers and decreased antioxidant capacity of the corneal cells,[48–52] as well as dysregulation of proinflammatory/anti-inflammatory interleukins, and immunity molecules, suggesting its potential role in the early cell death and degeneration in the corneal tissue.[53–56]

In a global overview, our study revealed the dysregulation of 15 proteins in the tear samples of KC offspring, some of them previously associated with the KC pathophysiology events, such as oxidative stress, inflammation, cell adhesion, cell/cell interaction, cell division and migration, and apoptosis. In the same way, results provided by the qualitative approach showed that the proteins exclusively identified in each O-KC group were also associated with the enrichment of oxidative, apoptosis, and structural processes.

First, the link with oxidative stress conditions was evidenced by the downregulation of several proteins such as lipocalin-1 (LCN-1), lactoferrin (LF), superoxide dismutase (SOD1), and peroxiredoxin-1 (PRDX1), which have essential roles in the protection against free radicals. LCN-1 was the most downregulated protein in the O-KC samples. Given the multifunctionality of this protein and its ability to clean up toxic ligands, LCN-1 is considered an essential member of cellular defense in epithelial tissues that combat oxidative stress.[57] In particular, previous studies have demonstrated the efficacy of LCN-1 as a physiological scavenger of harmful lipophilic molecules resulting from lipid peroxidation processes. Dysregulation of LCN-1 was previously observed in tear samples of KC patients, relating its overexpression to the need for oxidative protection during KC disease.[58,59] In this regard, the differences in study populations likely explain the variability in findings. This study is focused on the offspring of KC patients, with or without biomechanical alterations, so, our results suggest that LCN-1 deficiency may be linked to earlier disease stages or an increased KC susceptibility, contributing to ineffective protection against harmful species.

LF was the second most under-expressed protein in the study groups. Consistent with our findings, lower expression of LF in KC tear samples has been previously reported,[23,60,61] seeming to be related to the disease progression.[61] Because of its capability to regulate free iron levels in body fluids (by binding Fe^{3+} ions in the extracellular space) and to modulate and reduce the inflammatory and immunity responses,[61–63] LF underexpression could be associated with the oxidative-inflammatory microenvironment of KC pathophysiology. Our results showed that LF expression decreased as biomechanical properties indicated further weakening of the corneal tissue. In addition, LF had the highest sensitivity and specificity to discriminate between the controls and the O-KC biomechanically and tomographically healthy (O-KC-LR), and also the best AUC values for detecting the eyes with a high risk of ectasia development (O-KC-HR), suggesting its high potential to be a sensitive and specific biomarker for the detection of KC at-risk stages. Finally, SOD1 and PRDX1 levels also decreased in the O-KC groups compared to the control, with the lowest expression in groups with significant biomechanical impairment. Superoxide dismutases (SODs) are the primary defense systems for neutralizing free radicals and protecting against oxidative damage in cells.[64] Tear and serum samples of KC patients have shown a sharp decrease in the expression of SOD1, [50,65–67] and, due to the protective effect of this family of proteins in cells and tissues, the widespread argument suggests that downregulation of SOD1 could lead to an antioxidant defense failure in a tissue constantly exposed to high levels of UV radiation and highly vulnerable to oxidative damage. In the same way, peroxiredoxins (PRDXs) also represent an essential family of antioxidant enzymes with dominant functions in regulating and removing peroxide levels within cells.[68] Like SODs, PRDXs under-expression has been associated with the perturbation of tissue oxidative homeostasis and the activation of apoptotic pathways.[69] Genetic variations in *FOXO* (Forkhead box, class O) have been widely associated with KC disease,[70,71] as well as with corneal biomechanical behavior.[72] Specifically, the foxO family of transcription factors takes on a critical role in redox regulation and oxidative defense by promoting the transcription of genes encoding antioxidant proteins such as SODs and PRDXs.[73] Therefore the involvement and relevance of oxidative stress seem unquestionable, not only in the clinical evolution of KC but also associated with the risk of its development and the biomechanical imbalance.

In terms of mechanobiology and structural integrity, KC-related epithelial degeneration is characterized by alterations in superficial epithelial cell differentiation, abnormalities in basal epithelial density, and loss of its smoothness and regularity.[74,75] Similarly, abnormalities in stromal architecture are well documented, characterized by reduced keratocyte density and collagen fibers, resulting in a severe thinning of this layer.[19,76] The epithelium-stromal interaction is critical, and epithelial damage has been shown to induce cell death in surrounding stromal keratocytes,[77] suggesting that continued damage between the corneal epithelium and stroma constitutes an ongoing circle in the progressive thinning of corneal tissue during KC disease.[78] Corneal thickness is one of the most heritable human traits, with a strong genetic component and several associated genomic loci that account for its variability.[79] The functional implications of those genes are mainly related to collagen cross-linking, keratocyte growth and migration, epithelial proliferation and differentiation, and extracellular matrix organization.[79] In

this regard, we observed the dysregulation of five proteins in the O-KC samples (CFL1, CAPN1, EZN, ACNT4, and ACTG) involved in cell morphology and migration, cell/cell adhesion, cell/substrate binding, F-actin crosslinking, and cytoskeleton remodeling,[80-83] which may contribute to the onset of mechanical decline. CFL1, CAPN1, and EZN are required for the regulation of cell morphology, cell/substrate adhesion, cell/matrix networking, actin depolymerization, and cytoskeleton dynamics via integrin cell surface interactions, β-catenin signaling, RhoA or mTOR signaling pathways.[84,85] RhoA signaling is a highly conserved pathway involved in mechanotransduction in the corneal tissue; likewise, integrins and β-catenin play a vital role in focal adhesions and cytoskeletal adherences, so any impact affecting these pathways or components could weaken the cell/cell communication system.[86] CFL1 and CAPN1 dysregulation were previously observed in the stromal fibroblasts and epithelial cells of KC corneas, and changes in the expression of these proteins have been recognized as possible underlying factors of stromal thinning and structural failure.[78,87] In addition, we observed the downregulation of ACTN4, an F-actin cross-linking protein involved in the tight junctions of epithelial cells,[88] and ACTG, a member of the actin filaments. Despite no significant differences among O-KC groups in ACTN4 and ACRG expression, both proteins showed a decreased trend as the corneal biomechanical behavior weakened. Previous studies also reported alterations in the actin processes in KC, demonstrating the reduced expression of the β-actin encoding gene in human corneas with KC and suggesting that stromal keratocyte depletion may contribute to reduced β-actin expression, leading to cytoskeletal disruption and eventually stromal thinning and weakening.[89,90]

In connection with the pathological events affecting extracellular matrix during KC disease, we observed that SSA1 expression was significantly reduced in the O-KC-LR and O-KC-MR groups compared to the controls. KC fibroblasts have shown a deficiency in arginine and spermidine concentrations,[91,92] and even the benefits of supplementation with arginine have been postulated as a potential therapy for KC through its capacity to promote collagen type I production and increase extracellular matrix deposition.[91] As responsible for arginine biosynthesis in most body tissues, down-regulation of ASS1 could be associated with the arginine deficiency in KC disease.

Finally, regarding the overexpression of APOA2 in the O-KC groups, previous studies reported alterations in APOA1 and APOA2 levels in the tear samples and aqueous humor of KC patients.[93,94] Because of its involvement in lipid metabolism, the dysregulation of these proteins could be related to lipid peroxidation and imbalance, however, further studies are needed to understand the role of these proteins in biomechanical dysfunction and corneal ectasia.

Considering that the dysregulation of most structural proteins was observed even before detecting clinical alterations in the corneal biomechanical behavior of O-KC participants, our results seem consistent with a structural disturbance that even precedes the corneal weakening that can be detected with the current clinical biomechanical tools.

Beyond the specific biological impact on KC pathophysiology of the dysregulated proteins, LRA modeling determined the best biomarker combinations to discriminate between the control and the three O-KC groups, creating three specific protein panels with high sensitivity and specificity. In this sense, protein panels for KC risk assessment could enable the development of cost-effective early diagnosis and screening methods, avoiding extensive and expensive analyses (such as the global mass spectrometry proteomic analysis), and promoting the crossing from bench to clinic.

This is an innovative study marking the first attempt to identify the proteomic alterations linked to the risk of developing KC and those underlying the biomechanical decline associated with this disease; however, we have identified some limitations. The first one acknowledges that the subcategorization of the O-KC led to an uneven distribution of participants across the study groups. To address this limitation, future studies should include larger cohorts in the groups with smaller sample sizes (e.g., O-KC-HR group). Second, this study did not include a follow-up of the O-KC participants, so it seems desirable to design future prospective cohort studies to assess the evolution of these markers in those subjects who may develop clinical disease, a task we are currently working on. Furthermore, the variability of the tear proteome in different environmental and genetic backgrounds suggests the need to validate our results in diverse populations and larger cohorts. As well, integrating genetic studies will strengthen and complement our findings. Although this study offers novel clinical evidence of potential tear proteomic biomarkers linked to corneal biomechanical impairment and early KC, comprehensive in vitro studies are crucial to validate their significance in the pathological corneal biomechanical weakness.

In summary, the proteomic approach of this study emphasizes the relevance of some target proteins previously recognized to have a significant role in clinical KC, indicating their involvement in the disease's early and at-risk stages. In this sense, the high sensitivity and specificity of LCN1, LF, SOD1, EZN, and CAPN1 for detecting biomechanical alterations of corneal tissue make them promising biomarkers in the early detection of KC. Oxidative stress and cell structural alterations appear to begin long before the onset of clinical signs and even before alterations in the corneal biomechanics can be detected with the current tools. A thorough insight into the interplay between oxidative and structural events influencing cellular mechanobiology is required to develop effective therapeutic strategies for early KC management.

Acknowledgments

The authors thank all the participants involved in this study, as well as OCULUS Iberia S.L. for their collaboration in providing the biomechanics and tomography devices required for this work.

Supported by the Instituto de Salud Carlos III (ISCIII), cofinanced by the European Union (EU) (PI23/00323) and the Xunta de Galicia (Conselleria de Economía e Industria: IN607A2022/03 with the following ones.

Funded by Instituto de Salud Carlos III (ISCIII) through the project "PI23/00323" and co-funded by the European Union. The Xunta de Galicia also co-financed this study through the project IN607A2022/03.

M.L.L. acknowledges financial support from a predoctoral fellowship of Universidade de Santiago de Compostela and Banco Santander. Similarly, U.R. recognizes the support from Xunta de Galicia (Galician Innovation Agency GAIN: IN606C-

2024/003) postdoctoral fellowship. The funders had no role in the study design, data collection and analysis, decision to publish, or preparation of the manuscript.

Disclosure: **M. López-López**, None; **U. Regueiro**, None; **S. Bravo**, None; **C. Pena**, None; **Y. Pastoriza**, None; **M. Conde-Amboage**, None; **P. Hervella**, None; **I. Lema**, None

References

1. Belin MW, Asota IM, Ambrosio R, Khachikian SS. What's in a name: keratoconus, pellucid marginal degeneration, and related thinning disorders. *Am J Ophthalmol*. 2011;152:157–162.
2. Wagner H, Barr JT, Zadnik K. Collaborative Longitudinal Evaluation of Keratoconus (CLEK) study: methods and findings to date. *Cont Lens Anterior Eye*. 2007;30:223–232.
3. Ertan A, Muftuoglu O. Keratoconus clinical findings according to different age and gender groups. *Cornea*. 2008;27:1109–1113.
4. Li X, Yang H, Rabinowitz YS. Longitudinal study of keratoconus progression. *Exp Eye Res.* 2007;85:502–507.
5. Léoni-Mesplié S, Mortemousque B, Touboul D, et al. Scalability and severity of keratoconus in children. *Am J Ophthalmol*. 2012;154:56–62.
6. Gordon-Shaag A, Millodot M, Kaiserman I, et al. Risk factors for keratoconus in Israel: a case-control study. *Ophthalmic Physiol Opt*. 2015;35:673–681.
7. Keel S, Lingham G, Misra N, et al. Toward universal eye health coverage—key outcomes of the World Health Organization Package of Eye Care Interventions: a systematic review. *JAMA Ophthalmol*. 2022;140:1229–1238.
8. Vinciguerra R, Ambrósio R, Elsheikh A, et al. Detection of keratoconus with a new biomechanical index. *J Refract Surg*. 2016;32:803–810.
9. Scarcelli G, Besner S, Pineda R, Yun SH. Biomechanical characterization of keratoconus corneas ex vivo with Brillouin microscopy. *Invest Ophthalmol Vis Sci*. 2014;55:4490–4495.
10. Bykhovskaya Y, Rabinowitz YS. Update on the genetics of keratoconus. *Exp Eye Res*. 2021;202:108398.
11. Tuft SJ, Hassan H, George S, Frazer DG, Willoughby CE, Liskova P. Keratoconus in 18 pairs of twins. *Acta Ophthalmol*. 2012;90:482–486.
12. Weed KH, MacEwen CJ, McGhee CNJ. The variable expression of keratoconus within monozygotic twins: Dundee University Scottish Keratoconus Study (DUSKS). *Contact Lens Anterior Eye*. 2006;29:123–126.
13. Mathan JJ, Gokul A, Simkin SK, Meyer JJ, Patel DV, McGhee CNJ. Topographic screening reveals keratoconus to be extremely common in Down syndrome. *Clin Exp Ophthalmol*. 2020;48:1160–1167.
14. Vincent AL, Weiser BA, Cupryn M, Stein RM, Abdolell M, Levin AV. Computerized corneal topography in a paediatric population with Down syndrome. *Clin Exp Ophthalmol*. 2005;33:47–52.
15. Robertson I. Keratoconus and the Ehlers-Danlos syndrome: a new aspect of keratoconus. *Med J Aust*. 1975;1:571–573.
16. Elder MJ. Leber congenital amaurosis and its association with keratoconus and keratoglobus. *J Pediatr Ophthalmol Strabismus*. 1994;31:38–40.
17. Hameed A, Khaliq S, Ismail M, et al. A novel locus for Leber congenital amaurosis (LCA4) with anterior keratoconus mapping to chromosome 17p13. *Invest Ophthalmol Vis Sci*. 2000;41:629–633.
18. Olivo-Payne A, Abdala-Figuerola A, Hernandez-Bogantes E, Pedro-Aguilar L, Chan E, Godefrooij D. Optimal management of pediatric keratoconus: challenges and solutions. *Clin Ophthalmol*. 2019;13:1183–1191.
19. Santodomingo-Rubido J, Carracedo G, Suzaki A, Villa-Collar C, Vincent SJ, Wolffsohn JS. Keratoconus: an updated review. *Cont Lens Anterior Eye*. 2022;45(3):101559.
20. Awwad ST, Yehia M, Mehanna CJ, et al. Tomographic and refractive characteristics of pediatric first-degree relatives of keratoconus patients. *Am J Ophthalmol*. 2019;207:71–76.
21. Naderan M, Rajabi MT, Zarrinbakhsh P, Naderan M, Bakhshi A. Association between family history and keratoconus severity. *Curr Eye Res*. 2016;41:1414–1418.
22. Lema I, Duran J. Inflammatory molecules in the tears of patients with keratoconus. *Ophthalmology*. 2005;112:654–659.
23. Lema I, Brea D, Rodríguez-González R, Díez-Feijoo E, Sobrino T. Proteomic analysis of the tear film in patients with keratoconus. *Mol Vis*. 2010;16:2055–2061.
24. Balasubramanian SA, Wasinger VC, Pye DC, Willcox MD. Preliminary identification of differentially expressed tear proteins in keratoconus. *Mol Vis*. 2013;19:2124–2134.
25. López-López M, Regueiro U, Bravo S, et al. Tear proteomics in keratoconus: a quantitative SWATH-MS analysis. *Invest Ophthalmol Vis Sci*. 2021;62(10):30–30.
26. López-López M, Regueiro U, Bravo SB, et al. Shotgun proteomics for the identification and profiling of the tear proteome of keratoconus patients. *Invest Ophthalmol Vis Sci*. 2022;63(5): 12–12.
27. Efron N. Grading scales for contact lens complications. *Ophthalmic Physiol Opt*. 1998;18:182–186.
28. Chantada-Vázquez MDP, García Vence M, Serna A, Núñez C, Bravo SB. SWATH-MS protocols in human diseases. *Methods Mol Biol*. 2021;2259:105–141.
29. Bonzon-Kulichenko E, Pérez-Hernández D, Núñez E, et al. A robust method for quantitative high-throughput analysis of proteomes by 18O labeling. *Mol Cell Proteomics*. 2011;10(1):M110.003335.
30. Perez-Hernandez D, Gutiérrez-Vázquez C, Jorge I, et al. The intracellular interactome of tetraspanin-enriched microdomains reveals their function as sorting machinery toward exosomes. *J Biol Chem*. 2013;288:11649–11661.
31. Lapeyre G, Fournie P, Vernet R, et al. Keratoconus prevalence in families: a French study. *Cornea*. 2020;39:1473–1479.
32. Karimian F, Aramesh S, Rabei HM, Javadi MA, Rafati N. Topographic evaluation of relatives of patients with keratoconus. *Cornea*. 2008;27:874–878.
33. Kaya V, Utine CA, Altunsoy M, Oral D, Yilmaz OF. Evaluation of corneal topography with Orbscan II in first-degree relatives of patients with keratoconus. *Cornea*. 2008;27(5):531–534.
34. Shneor E, Frucht-Pery J, Granit E, Gordon-Shaag A. The prevalence of corneal abnormalities in first-degree relatives of patients with keratoconus: a prospective case-control study. *Ophthalmic Physiol Opt*. 2020;40:442.
35. Kara N, Altinkaynak H, Baz O, Goker Y. Biomechanical evaluation of cornea in topographically normal relatives of patients with keratoconus. *Cornea*. 2013;32:262–266.
36. Ionescu IC, Corbu CG, Tanase C, et al. Overexpression of tear inflammatory cytokines as additional findings in keratoconus patients and their first degree family members. *Mediators Inflamm*. 2018;2018:4285268.
37. Regueiro U, López-López M, Hervella P, Sobrino T, Lema I. Corneal and conjunctival alteration of innate immune expression in first-degree relatives of keratoconus patients. *Graefes Arch Clin Exp Ophthalmol*. 2021;259:459–467
38. Shinde V, Sobreira N, Wohler ES, et al. Pathogenic alleles in microtubule, secretory granule and extracellular matrix-related genes in familial keratoconus. *Hum Mol Genet*. 2021;30:658–671.

Investigative Ophthalmology & Visual Science

39. Tian L, Zhang D, Guo L, et al. Comparisons of corneal biomechanical and tomographic parameters among thin normal cornea, forme fruste keratoconus, and mild keratoconus. *Eye Vis (Lond)*. 2021;8:44.
40. Wang YM, Chan TCY, Yu M, Jhanji V. Comparison of corneal dynamic and tomographic analysis in normal, forme fruste keratoconic, and keratoconic eyes. *J Refract Surg*. 2017;33:632–638.
41. Ionescu IC, Corbu CG, Nicula C, et al. The importance of corneal biomechanics in assessing first degree family members of keratoconus patients. *Rom J Ophthalmol*. 2018;62:149–154.
42. Sedaghat MR, Momeni-Moghaddam H, Ehsaei A, Vinciguerra R, Zamani O, Robabi H. Comparison of corneal biomechanical properties in healthy thin corneas with matched keratoconus eyes. *J Cataract Refract Surg*. 2023;49:234–238.
43. Ambrósio R, Alonso RS, Luz A, Coca Velarde LG. Corneal-thickness spatial profile and corneal-volume distribution: tomographic indices to detect keratoconus. *J Cataract Refract Surg*. 2006;32:1851–1859.
44. Ambrósio R, Caiado ALC, Guerra FP, et al. Novel pachymetric parameters based on corneal tomography for diagnosing keratoconus. *J Refract Surg*. 2011;27:753–758.
45. Song P, Yang K, Li P, et al. Assessment of corneal pachymetry distribution and morphologic changes in subclinical keratoconus with normal biomechanics. *Biomed Res Int*. 2019;2019(1):1748579.
46. Lema I, Sobrino T, Duran JA, Brea D, Diez-Feijoo E. Subclinical keratoconus and inflammatory molecules from tears. *Br J Ophthalmol*. 2009;93:820–824.
47. di Martino E, Ali M, Inglehearn CF. Matrix metalloproteinases in keratoconus—too much of a good thing?. *Exp Eye Res*. 2019;182:137–143.
48. Shetty R, Sharma A, Pahuja N, et al. Oxidative stress induces dysregulated autophagy in corneal epithelium of keratoconus patients. *PLoS One*. 2017;12(9):1–20.
49. Chwa M, Atilano SR, Hertzog D, et al. Hypersensitive response to oxidative stress in keratoconus corneal fibroblasts. *Invest Ophthalmol Vis Sci*. 2008;49:4361–4369.
50. Atilano S, Lee D, Fukuhara P, et al. Corneal oxidative damage in keratoconus cells due to decreased oxidant elimination from modified expression levels of SOD enzymes, PRDX6, SCARA3, CPSF3, and FOXM1. *J Ophthalmic Vis Res*. 2019;14:62–70.
51. Navel V, Malecaze J, Pereira B, et al. Oxidative and antioxidative stress markers in keratoconus: a systematic review and meta-analysis. *Acta Ophthalmol*. 2021;99(6):e777–e794.
52. Shinde V, Hu N, Mahale A, et al. RNA sequencing of corneas from two keratoconus patient groups identifies potential biomarkers and decreased NRF2-antioxidant responses. *Sci Rep*. 2020;10(1):9907.
53. Balasubramanian SA, Mohan S, Pye DC, Willcox MD. Proteases, proteolysis, and inflammatory molecules in the tears of people with keratoconus. *Acta Ophthalmol*. 2012;90(4):e303–e309.
54. Malfeito M, Regueiro U, Pérez-Mato M, Campos F, Sobrino T, Lema I. Innate Immunity Biomarkers for Early Detection of Keratoconus. *Ocul Immunol Inflamm*. 2019;27:942–948.
55. Lema I, Durán JA, Ruiz C, Díez-Feijoo E, Acera A, Merayo J. Inflammatory response to contact lenses in patients with keratoconus compared with myopic subjects. *Cornea*. 2008;27:758–763.
56. Jun AS, Cope L, Speck C, et al. Subnormal cytokine profile in the tear fluid of keratoconus patients. *PLoS One*. 2011;6(1):e16437.
57. Lechner M, Wojnar P, Redl B. Human tear lipocalin acts as an oxidative-stress-induced scavenger of potentially harmful lipid peroxidation products in a cell culture system. *Biochem J*. 2001;356(Pt 1):129–135.
58. Pannebaker C, Chandler HL, Nichols JJ. Tear proteomics in keratoconus. *Mol Vis*. 2010;16:1949–1957.
59. Acera A, Vecino E, Rodríguez-Agirretxe I, et al. Changes in tear protein profile in keratoconus disease. *Eye*. 2011;25:1225–1233.
60. Balasubramanian SA, Pye DC, Willcox MD. Levels of lactoferrin, secretory IgA and serum albumin in the tear film of people with keratoconus. *Exp Eye Res*. 2012;96:132–137.
61. Regueiro U, López-López M, Varela-Fernández R, Sobrino T, Diez-Feijoo E, Lema I. Immunomodulatory effect of human lactoferrin on toll-like receptors 2 expression as therapeutic approach for keratoconus. *Int J Mol Sci*. 2022;23:12350.
62. Rosa L, Cutone A, Lepanto MS, Paesano R, Valenti P. Lactoferrin: A Natural Glycoprotein Involved in Iron and Inflammatory Homeostasis. *Int J Mol Sci*. 2017;18:1985.
63. Regueiro U, López-López M, Varela-Fernández R, Otero-Espinar FJ, Lema I. Biomedical applications of lactoferrin on the ocular surface. *Pharmaceutics*. 2023;15:865.
64. Nozik-Grayck E, Suliman HB, Piantadosi CA. Extracellular superoxide dismutase. *Int J Biochem Cell Biol*. 2005;37:2466–2471.
65. Tekin S, Seven E. Assessment of serum catalase, reduced glutathione, and superoxide dismutase activities and malondialdehyde levels in keratoconus patients. *Eye (Lond)*. 2022;36:2062–2066.
66. Balmus IM, Alexa AI, Ciuntu RE, et al. Oxidative stress markers dynamics in keratoconus patients' tears before and after corneal collagen crosslinking procedure. *Exp Eye Res*. 2020;190:107897.
67. Udar N, Atilano SR, Brown DJ, et al. SOD1: a candidate gene for keratoconus. *Invest Ophthalmol Vis Sci*. 2006;47:3345–3351.
68. Perkins A, Nelson KJ, Parsonage D, Poole LB, Karplus PA. Peroxiredoxins: guardians against oxidative stress and modulators of peroxide signaling. *Trends Biochem Sci*. 2015;40:435.
69. Wojcik K, Kaminska A, Blasiak J, Szaflik J, Szaflik JP. Oxidative stress in the pathogenesis of Keratoconus and Fuchs endothelial corneal dystrophy. *Int J Mol Sci*. 2013;14:19294–19308.
70. Liskova P, Dudakova L, Krepelova A, Klema J, Hysi PG. Replication of SNP associations with keratoconus in a Czech cohort. *PLoS One*. 2017;12(2):e0172365.
71. Lu Y, Vitart V, Burdon KP, et al. Genome-wide association analyses identify multiple loci associated with central corneal thickness and keratoconus. *Nat Genet*. 2013;45:155–163.
72. Khawaja AP, Rojas Lopez KE, Hardcastle AJ, et al. Genetic variants associated with corneal biomechanical properties and potentially conferring susceptibility to keratoconus in a genome-wide association study. *JAMA Ophthalmol*. 2019;137:1005–1012.
73. Klotz LO, Sánchez-Ramos C, Prieto-Arroyo I, Urbánek P, Steinbrenner H, Monsalve M. Redox regulation of FoxO transcription factors. *Redox Biol*. 2015;6:51–72.
74. Jongebloed WL, Worst JF. The keratoconus epithelium studied by SEM. *Doc Ophthalmol*. 1987;67(1-2):171–181.
75. Efron N, Hollingsworth JG. New perspectives on keratoconus as revealed by corneal confocal microscopy. *Clin Exp Optom*. 2008;91:34–55.
76. Sykakis E, Carley F, Irion L, Denton J, Hillarby MC. An in-depth analysis of histopathological characteristics found in keratoconus. *Pathology*. 2012;44:234–239.
77. Wilson SE, He YG, Weng J, et al. Epithelial injury induces keratocyte apoptosis: hypothesized role for the interleukin-1 system in the modulation of corneal tissue organi-

Investigative Ophthalmology & Visual Science

zation and wound healing. *Exp Eye Res*. 1996;62:325–327.

78. Lee JE, Oum BS, Choi HY, Lee SU, Lee JS. Evaluation of differentially expressed genes identified in keratoconus. *Mol Vis*. 2009;15:2480–2487.
79. Choquet H, Melles RB, Yin J, et al. A multiethnic genome-wide analysis of 44,039 individuals identifies 41 new loci associated with central corneal thickness. *Commun Biol*. 2020;3:301.
80. Bernstein BW, Bamburg JR. ADF/Cofilin: a functional node in cell biology. *Trends Cell Biol*. 2010;20(4):187.
81. Wells A, Huttenlocher A, Lauffenburger DA. Calpain proteases in cell adhesion and motility. *Int Rev Cytol*. 2005;245:1–16.
82. Hoskin V, Szeto A, Ghaffari A, Greer PA, CÃtéc GP, Elliott BE. Ezrin regulates focal adhesion and invadopodia dynamics by altering calpain activity to promote breast cancer cell invasion. *Mol Biol Cell*. 2015;26:3464–3479.
83. Shao H, Wang JH, Pollak MR, Wells A. α-actinin-4 is essential for maintaining the spreading, motility and contractility of fibroblasts. *PLoS One*. 2010;5(11):e13921.
84. Kulkarni S, Saido TC, Suzuki K, Fox JEB. Calpain mediates integrin-induced signaling at a point upstream of Rho family members. *J Biol Chem*. 1999;274:21265–21275.
85. Hiscox S, Jiang WG. Ezrin regulates cell-cell and cell-matrix adhesion, a possible role with E-cadherin/beta-catenin. *J Cell Sci*. 1999;112(Pt 18):3081–3090.
86. Thomasy SM, Leonard BC, Greiner MA, Skeie JM, Raghunathan VK. Squishy matters—corneal mechanobiology in health and disease. *Prog Retin Eye Res*. 2024;99:101234.
87. Joseph R, Srivastava OP, Pfister RR. Differential epithelial and stromal protein profiles in keratoconus and normal human corneas. *Exp Eye Res*. 2011;92:282–298.
88. Otey CA, Carpen O. Alpha-actinin revisited: a fresh look at an old player. *Cell Motil Cytoskeleton*. 2004;58:104–111.
89. Macé M, Galiacy SD, Erraud A, et al. Comparative transcriptome and network biology analyses demonstrate antiproliferative and hyperapoptotic phenotypes in human keratoconus corneas. *Invest Ophthalmol Vis Sci*. 2011;52:6181–6191.
90. Khaled ML, Helwa I, Drewry M, Seremwe M, Estes A, Liu Y. Molecular and histopathological changes associated with keratoconus. *Biomed Res Int*. 2017;2017:7803029.
91. McKay TB, Priyadarsini S, Rowsey T, Karamichos D. Arginine supplementation promotes extracellular matrix and metabolic changes in keratoconus. *Cells*. 2021;10:2076.
92. Stachon T, Kolev K, Flaskó Z, Seitz B, Langenbucher A, Szentmáry N. Arginase activity, urea, and hydroxyproline concentration are reduced in keratoconus keratocytes. *Graefes Arch Clin Exp Ophthalmol*. 2017;255:91–97.
93. Soria J, Villarrubia A, Merayo-Lloves J, et al. Label-free LC-MS/MS quantitative analysis of aqueous humor from keratoconic and normal eyes. *Mol Vis*. 2015;21:451–460.
94. Yenihayat F, Altıntaş Ö, Kasap M, Akpınar G, Güzel N, Çelik OS. Comparative proteome analysis of the tear samples in patients with low-grade keratoconus. *Int Ophthalmol*. 2018;38:1895–1905.

Investigative Ophthalmology & Visual Science